Shifts and widths of collective excitations in trapped Bose gases determined by the dielectric formalism

Jürgen Reidl,[1] András Csordás,[2] Robert Graham,[1] and Péter Szépfalusy[3]
[1]*Fachbereich Physik, Universität Gesamthochschule Essen, 45117 Essen, Germany*
[2]*Research Group for Statistical Physics of the Hungarian Academy of Sciences, Pázmány Péter sétány 1/A, H-1117 Budapest, Hungary*
[3]*Department of Physics of Complex Systems, Eötvös University, Pázmány Péter sétány 1/A, H-1117 Budapest, Hungary and Research Institute for Solid State Physics and Optics, P.O. Box 49, H-1525 Budapest, Hungary*
(Received 27 September 1999; published 10 March 2000)

We present predictions for temperature-dependent shifts and damping rates. They are obtained by applying the dielectric formalism to set up a self-consistent model of a trapped Bose gas which can be shown to satisfy generalized Ward identities. Within the framework of the model we use lowest-order perturbation theory to determine the first-order correction to the results of Hartree-Fock-Bogoliubov-Popov theory for the complex collective excitation frequencies, and present numerical results for the temperature dependence of the damping rates and the frequency shifts. Good agreement with the experimental values measured by Jin *et al.* [Phys. Rev. Lett. **77**, 420 (1996)] are found for the $m=2$ mode, while we find disagreements in the shifts for $m=0$. The latter point to the necessity of a nonperturbative treatment for an explanation of the temperature dependence of the $m=0$ shifts.

PACS number(s): 03.75.Fi, 05.30.Jp, 67.40.Db

I. INTRODUCTION

Since the discovery of Bose-Einstein condensation in traps, a wealth of experimental data on collective excitations has appeared in the literature (for experimental reviews, see Refs. [1,2]) waiting for theoretical explanation. Some of the earliest measurements, still requiring a firm theoretical analysis, were performed in oscillating traps which permitted a selective excitation of different excitation modes [3–6]. Common features of the above experiments are that the density of atoms in the trap is relatively small and the temperature is extremely low. Consequently, from the theoretical point of view the atoms can be treated as a weakly interacting degenerate Bose gas, while the interaction potential is well described by the *s*-wave approximation. Due to the presence of the trap the whole system is not translationally invariant, and field equations of any approximation must be solved in real space, not in momentum space. Furthermore the excitation spectrum is discrete rather than continuous as in spatially homogeneous condensates like He II.

Nevertheless, most theoretical approaches are based on the natural generalization of one or the other of the homogeneous descriptions to the inhomogeneous case. The present paper also holds to this line. It is based on the dielectric formalism (see Ref. [7] and further references therein), first introduced for spatially homogeneous systems at zero temperature [8–10], later used at finite temperature [11,12], and recently generalized to inhomogeneous systems in Ref. [13]. The great success of the dielectric formalism lies in showing that the order parameter correlation function (the one-particle Green's function) and the density-density correlation function have the same spectra below the critical temperature. In principle the dielectric formalism is valid at all temperatures, but still requires one to deal with infinitely many graphs to obtain exact results. In practice, however, one resorts to some approximations for the proper and irreducible part of certain quantities of physical interest, which are the key quantities in the dielectric formalism. Following and extending Refs. [11,13], we shall base our investigation on a simple model for trapped weakly interacting Bose gases, which in homogeneous systems (a) is valid at finite temperature, (b) satisfies the generalized Ward identities, and (c) guarantees that both the Green's function and the density-density autocorrelation spectra exhibit the same excitations. In addition the model we use, which builds on and extends a simpler one discussed in detail in Refs. [11,7], can be shown to be related to an approximation used by Minguzzi and Tosi [14].

It is our main purpose here to evaluate, within the approximation defined by our choice of the model, the damping rates and frequency shifts and to compare the results with the experimental data of Jin *et al.* [4]. In principle we are also able to calculate theoretical values for the MIT measurement, but in our present approach we treat the fluctuations of the thermal density perturbatively and consider only Landau damping. This approach is justified if the condition $k_BT \gg \mu$ is fulfilled which is only the case for the JILA measurements. Furthermore, the high anisotropy of the MIT trap leads to some numerical difficulties in the code we use so far. From the theoretical side several papers have appeared in the literature going beyond the Hartree-Fock-Bogoliubov-Popov (HFBP) approximation [15], which is really necessary to take into account damping processes. Most relevant papers beyond that approximation describe the damping process [16–21] or calculate the shifts by including the anomalous average in such a way that the resulting approximation is gapless [22]. The approach applied in Ref. [21] is the second-order Beliaev theory which is known to be gapless. It treats both Beliaev and Landau dampings, and also calculates the shift of elementary excitations in local density approximation along with their damping.

In the present paper we wish to present a theory of the shifts and widths of the *low-lying* modes. Our approach is based on the dielectric formalism, and achieves its simplicity

by a judicious selection of a subset of graphs for the *proper part* of the physical quantities of interest. The model we shall investigate in detail in this work accounts for the Landau damping, but cannot account for Beliaev damping. This sacrifice for gain in simplicity is not too large because in the temperature region where the measurements we wish to understand are performed, and where we calculate the shifts and the damping rates, the Beliaev damping of the excitations is negligible.

The paper is organized as follows. In Sec. II we briefly summarize the general framework of the dielectric formalism for inhomogeneous systems, and consider an extended version of the model approximation of Refs. [11,13]. The conditions for choosing the necessary basic building blocks for the ladder approximation and for the proper and irreducible quantities are spelled out. Then the quantities given in our formalism are related to the fluctuations of the condensate and the thermal density. We show that neglecting the thermal density fluctuations we recover the usual Hartree-Fock-Bogoliubov-Popov equations [15]. Then we derive the corrections of the HFBP excitation energies to first order in the thermal density fluctuations. To solve the closed set of equations for the damping and the shifts still requires some numerical work in the inhomogeneous case. We briefly discuss our numerical procedure in Sec. III. Section IV contains a discussion of our results, and a comparison with the experimental data measured at JILA. Section V is devoted to conclusions and to some final remarks. There we also compare our model approximation with other approximations given in the literature, e.g., the already mentioned treatment of all the Beliaev diagrams by Shi and Griffin [16] and Fedichev and Shlyapnikov [21], the kinetic equations of Ref. [14] and the collisionless Boltzmann equation [23,24].

II. FORMULATION

Here we summarize the dielectric formalism first applied to inhomogeneous systems in Ref. [13]. However, we shall not repeat the whole treatment, but rather concentrate on the key points, and indicate further steps.

The Hamiltonian of our problem in second quantized form, is

$$\hat{H}=\int d^3r\,\hat{\Psi}^\dagger(\boldsymbol{r})\left(-\frac{\hbar^2}{2m}\Delta+U(\boldsymbol{r})\right)\hat{\Psi}(\boldsymbol{r}) + \frac{1}{2}\int d^3r_1\int d^3r_2\,\hat{\Psi}^\dagger(\boldsymbol{r}_1)\hat{\Psi}^\dagger(\boldsymbol{r}_2)v(\boldsymbol{r}_1,\boldsymbol{r}_2)\hat{\Psi}(\boldsymbol{r}_1)\hat{\Psi}(\boldsymbol{r}_2), \tag{1}$$

where $\hat{\Psi}(\boldsymbol{r})$ is the Bose field operator, $U(\boldsymbol{r})$ is the trap potential, and $v(\boldsymbol{r}_1,\boldsymbol{r}_2)$ describes the two-body interaction. In the following, this is chosen as

$$v(\boldsymbol{r},\boldsymbol{r}')=g\,\delta(\boldsymbol{r}-\boldsymbol{r}')\equiv\frac{4\pi\hbar^2 a}{m}\,\delta(\boldsymbol{r}-\boldsymbol{r}'), \tag{2}$$

where a is the s-wave scattering length and m is the mass of the atoms. Throughout we shall restrict ourselves to temperatures below the critical temperature. As usual, for $T<T_c$ we split off the condensate wave function $\Phi_0(\boldsymbol{r})$,

$$\hat{\Psi}(\boldsymbol{r})=\Phi_0(\boldsymbol{r})+\hat{\Phi}(\boldsymbol{r}), \tag{3}$$

where $\Phi_0(\boldsymbol{r})=\langle\hat{\Psi}(\boldsymbol{r})\rangle$, and $\langle\cdots\rangle$ denotes thermal averaging

$$\langle\hat{A}\rangle=\frac{\mathrm{Tr}\,\hat{A}e^{-\beta(\hat{H}-\mu\hat{N})}}{\mathrm{Tr}\,e^{-\beta(\hat{H}-\mu\hat{N})}}. \tag{4}$$

Since we are interested in finite-temperature excitations, we use Green's functions

$$G_{\alpha,\beta}(\boldsymbol{r},\tau;\boldsymbol{r}',\tau')=-\langle T_\tau[\hat{\Phi}_\alpha(\boldsymbol{r},\tau)\hat{\Phi}^\dagger_\beta(\boldsymbol{r}',\tau')]\rangle, \tag{5}$$

with field operators in Matsubara representation $\hat{\Phi}_1(\boldsymbol{r},\tau)\equiv\hat{\Phi}(\boldsymbol{r},\tau)$ and $\hat{\Phi}_2(\boldsymbol{r},\tau)\equiv\hat{\Phi}^\dagger(\boldsymbol{r},\tau)$. The other key quantity we are interested in is the density autocorrelation function

$$\chi(\boldsymbol{r},\tau;\boldsymbol{r}',\tau')=-\langle T_\tau[\tilde{n}(\boldsymbol{r},\tau)\tilde{n}(\boldsymbol{r}',\tau')]\rangle, \tag{6}$$

where $\tilde{n}(\boldsymbol{r})=\hat{n}(\boldsymbol{r})-\langle\hat{n}(\boldsymbol{r})\rangle$. The finite temperature Green's functions (5) and the autocorrelation function (6) are functions of τ,τ' via $\tau-\tau'$ only and are periodic with period $\beta\hbar$. Thus one can expand them as Fourier series. The Matsubara Fourier coefficients are given by

$$G_{\alpha,\beta}(\boldsymbol{r},\boldsymbol{r}',i\omega_n)=\int_0^{\beta\hbar}d\tau\,e^{i\omega_n\tau}G_{\alpha,\beta}(\boldsymbol{r},\boldsymbol{r}',\tau), \qquad \omega_n=\frac{2n\pi}{\hbar\beta}, \tag{7}$$

where n is an integer. A corresponding expansion is made for $\chi(\boldsymbol{r},\tau;\boldsymbol{r}',\tau')$ with coefficients $\chi(\boldsymbol{r},\boldsymbol{r}',i\omega_n)$. Retarded functions can be obtained by the usual analytic continuation ($i\omega_n\to\omega+i\eta$, where η is infinitesimal).

It is useful to introduce the *proper part* of a quantity which is defined as *the sum of diagrammatic contributions, which cannot be split into two parts by cutting a single interaction line*. In the following proper parts will be denoted by a tilde. By definition the density autocorrelation function and its proper part fulfill

$$\chi(\boldsymbol{r},\boldsymbol{r}',\omega)=\tilde{\chi}(\boldsymbol{r},\boldsymbol{r}',\omega)+\frac{1}{\hbar}\int d^3r_1\int d^3r_2\,\tilde{\chi}(\boldsymbol{r},\boldsymbol{r}_1,\omega)v(\boldsymbol{r}_1,\boldsymbol{r}_2)\times\chi(\boldsymbol{r}_2,\boldsymbol{r}',\omega). \tag{8}$$

When $\chi(\boldsymbol{r},\boldsymbol{r}',\omega)$ has a pole in ω, but its proper part is nonsingular at the same ω, then there exists an eigenfunction $\xi(\boldsymbol{r})$ satisfying

$$\xi(\boldsymbol{r})=\frac{1}{\hbar}\int d^3r_1\int d^3r_2\,\tilde{\chi}(\boldsymbol{r},\boldsymbol{r}_1,\omega)v(\boldsymbol{r}_1,\boldsymbol{r}_2)\xi(\boldsymbol{r}_2). \tag{9}$$

This eigenfunction can be identified with the total density fluctuation $\delta n(\boldsymbol{r})=\xi(\boldsymbol{r})$ at the eigenfrequency given by the pole. In a similar way we obtain the eigenfunctions φ_1 and

φ_2, corresponding to the one-particle Green's functions $G_{\alpha,\beta}$, by solving the eigenproblem

$$\varphi_\alpha(\boldsymbol{r})=\frac{1}{\hbar}\int d^3\boldsymbol{r}_1\int d^3\boldsymbol{r}_2 G^{HO}_{\alpha,\gamma}(\boldsymbol{r},\boldsymbol{r}_1,\omega)\Sigma_{\gamma,\beta}(\boldsymbol{r}_1,\boldsymbol{r}_2,\omega)\varphi_\beta(\boldsymbol{r}_2). \tag{10}$$

(Here and in the following we adopt the convention that summation has to be taken over repeated greek indices.)

$$G^{HO}_{11}(\boldsymbol{r},\boldsymbol{r}',\omega_n)=G^{HO}_{22}(\boldsymbol{r}',\boldsymbol{r},-\omega_n)$$
$$=\sum_j \frac{\varphi^{HO}_j(\boldsymbol{r})\varphi^{HO}_j(\boldsymbol{r}')^*}{\omega_n-\hbar^{-1}(\epsilon^{HO}_j-\mu^{HO})},$$
$$G^{HO}_{12}(\boldsymbol{r},\boldsymbol{r}',\omega_n)=G^{HO}_{21}(\boldsymbol{r},\boldsymbol{r}',\omega_n)=0$$

are the Green's functions of the free harmonic trap with the corresponding harmonic oscillator excitation frequencies ϵ^{HO}_j, eigenfunctions $\varphi^{HO}_j(\boldsymbol{r})$, and chemical potential $\mu^{HO}=(\hbar/2)(\omega_x+\omega_y+\omega_z)$, where $\omega_{x,y,z}$ are the three trap frequencies. $\Sigma_{\alpha,\beta}$ are the self-energies describing the corrections due to the interactions. The condensate density fluctuations $\delta n_c(\boldsymbol{r})$ given by perturbations of the condensate density $n_c(\boldsymbol{r})=|\Phi_0(\boldsymbol{r})|^2$ due to excitations of single-quasiparticle modes can be identified with

$$\delta n_c(\boldsymbol{r})=\Phi_0(\boldsymbol{r})[\varphi_1(\boldsymbol{r})+\varphi_2(\boldsymbol{r})]. \tag{11}$$

Below T_c the proper part $\tilde{\chi}$ can be further decomposed into *irreducibile* (also termed ''regular'') $\tilde{\chi}^{(r)}$ and *reducible* (also termed ''singular'') $\tilde{\chi}^{(s)}$ parts. We call a diagram *irreducible* if *it cannot be split into two parts by cutting a single-particle line*. The reducible part $\tilde{\chi}^{(s)}$ is related to the existence of the so-called anomalous proper vertex $\tilde{\Lambda}_\alpha$, which contains all the proper diagrams with only one outer interaction line and only one outer particle line, and which is due to the presence of the condensate below T_c:

$$\tilde{\chi}(\boldsymbol{r},\boldsymbol{r}',\omega)=\tilde{\chi}^{(r)}(\boldsymbol{r},\boldsymbol{r}',\omega)+\tilde{\chi}^{(s)}(\boldsymbol{r},\boldsymbol{r}',\omega)$$
$$\tilde{\chi}^{(s)}(\boldsymbol{r},\boldsymbol{r}',\omega)=\int d^3r_1\int d^3r_2\,\tilde{\Lambda}_\alpha(\boldsymbol{r},\boldsymbol{r}_1,\omega)\tilde{G}_{\alpha,\beta}(\boldsymbol{r}_1,\boldsymbol{r}_2,\omega)$$
$$\times\tilde{\Lambda}_\beta(\boldsymbol{r}_2,\boldsymbol{r}',\omega). \tag{12}$$

Here $\tilde{G}_{\alpha,\beta}(\boldsymbol{r}_1,\boldsymbol{r}_2,\omega)$ is the proper part of the Green's function satisfying Dyson's equation with the proper part $\tilde{\Sigma}_{\alpha,\beta}(\boldsymbol{r}_1,\boldsymbol{r}_2,\omega)$ of the self-energy only. In Ref. [13] it is shown that the eigenfunctions ξ,φ_α belonging to the same eigenvalue ω are related by the anomalous vertex Λ_α containing all the proper and improper vertex contributions:

$$\xi(\boldsymbol{r})=\int d^3\boldsymbol{r}_1\,\Lambda_\alpha(\boldsymbol{r},\boldsymbol{r}_1,\omega)\varphi_\alpha(\boldsymbol{r}_1). \tag{13}$$

So far no approximation has been made. Now we define approximate expressions for the building blocks $\tilde{\Lambda}^0_\alpha$ and $\tilde{\chi}^0$ of the ladder approximation, in which we derive the proper quantities $\tilde{\Lambda}_\alpha$ and $\tilde{\chi}^{(r)}$: the trivial vertex function

$$\tilde{\Lambda}^0_1(\boldsymbol{r},\boldsymbol{r}',\omega)=\tilde{\Lambda}^0_2(\boldsymbol{r},\boldsymbol{r}',\omega)=\Phi_0(\boldsymbol{r})\,\delta(\boldsymbol{r}-\boldsymbol{r}'), \tag{14}$$

and the bubble graph

$$\tilde{\chi}^0(\boldsymbol{r},\boldsymbol{r}',\omega)=-\frac{1}{2\beta\hbar}\sum_n G^{HF}_{\alpha,\beta}(\boldsymbol{r},\boldsymbol{r}',i\omega_n)G^{HF}_{\beta,\alpha}(\boldsymbol{r}',\boldsymbol{r},i\omega_n-\omega)$$
$$=-\frac{1}{\beta\hbar}\sum_n G^{HF}_{1,1}(\boldsymbol{r},\boldsymbol{r}',i\omega_n)G^{HF}_{1,1}(\boldsymbol{r}',\boldsymbol{r},i\omega_n-\omega), \tag{15}$$

with the Green's function $G^{HF}_{\alpha,\beta}$ corresponding to the Hartree-Fock Hamiltonian

$$\hat{H}^{HF}(\boldsymbol{r})=-\frac{\hbar^2\nabla^2}{2m}+U(\boldsymbol{r})+2gn(\boldsymbol{r}). \tag{16}$$

The Green's functions $G^{HF}_{\alpha,\beta}$ satisfy the relations

$$[\hbar\omega-\hat{H}^{HF}(\boldsymbol{r})]G^{HF}_{11}(\boldsymbol{r},\boldsymbol{r}',\omega)=\hbar\,\delta(\boldsymbol{r}-\boldsymbol{r}'), \tag{17}$$
$$G^{HF}_{22}(\boldsymbol{r},\boldsymbol{r}',\omega)=G^{HF}_{11}(\boldsymbol{r}',\boldsymbol{r},-\omega), \tag{18}$$
$$G^{HF}_{12}=G^{HF}_{21}=0. \tag{19}$$

We have already used the Hartree-Fock Green's functions in the bubble graph. We will see later that this approach turns out to be consistent.

In the ladder approximation the proper contributions $\tilde{\chi}^{(r)}(\boldsymbol{r},\boldsymbol{r}',\omega)$ are derived by subsequent insertions of interaction lines into the bubble diagrams. Therefore, $\tilde{\chi}^{(r)}(\boldsymbol{r},\boldsymbol{r}',\omega)$ is determined by the self-consistent equation

$$\tilde{\chi}^{(r)}(\boldsymbol{r},\boldsymbol{r}',\omega)=\tilde{\chi}^0(\boldsymbol{r},\boldsymbol{r}',\omega)$$
$$+\frac{g}{\hbar}\int d^3\boldsymbol{r}_1\,\tilde{\chi}^0(\boldsymbol{r},\boldsymbol{r}_1,\omega)\tilde{\chi}^{(r)}(\boldsymbol{r}_1,\boldsymbol{r}',\omega). \tag{20}$$

For the proper vertex function $\tilde{\Lambda}_\alpha$ we take into account the trivial vertex $\tilde{\Lambda}^0_\alpha(\boldsymbol{r})$ and the first-order correction $\tilde{\Lambda}^{(1)}_\alpha(\boldsymbol{r},\boldsymbol{r}',\omega)=g\tilde{\chi}^0(\boldsymbol{r},\boldsymbol{r}',\omega)\Phi_0(\boldsymbol{r}')$. In $\tilde{\Lambda}^{(1)}_\alpha$ we replace the single interaction line by the T matrix which defines the following equation for the proper vertex function $\tilde{\Lambda}_\alpha$:

$$\tilde{\Lambda}_\alpha(\boldsymbol{r},\boldsymbol{r}',\omega)=\tilde{\Lambda}^0_\alpha(\boldsymbol{r},\boldsymbol{r}',\omega)$$
$$+\frac{g}{\hbar}\int d^3\boldsymbol{r}_1\,\tilde{\chi}^0(\boldsymbol{r},\boldsymbol{r}_1,\omega)\tilde{\Lambda}_\alpha(\boldsymbol{r}_1,\boldsymbol{r}',\omega), \tag{21}$$

from which it can be determined self-consistently.

The analogous Dyson equation for the complete vertex function given by $\Lambda_\alpha(\boldsymbol{r},\boldsymbol{r}',\omega)=\tilde{\Lambda}_\alpha(\boldsymbol{r},\boldsymbol{r}',\omega)$

$+(g/\hbar)\int d^3\boldsymbol{r}_1\,\tilde{\chi}^{(r)}(\boldsymbol{r},\boldsymbol{r}_1,\omega)\Lambda_\alpha(\boldsymbol{r}_1,\boldsymbol{r}',\omega)$ can be easily expressed in terms of the building blocks of the ladder approximation:

$$\Lambda_\alpha(\boldsymbol{r},\boldsymbol{r}',\omega)=\tilde{\Lambda}^0_\alpha(\boldsymbol{r},\boldsymbol{r}',\omega)+2\frac{g}{\hbar}\int d^3\boldsymbol{r}_1\,\tilde{\chi}^0(\boldsymbol{r},\boldsymbol{r}_1,\omega)\Lambda_\alpha(\boldsymbol{r}_1,\boldsymbol{r}',\omega). \tag{22}$$

We identify the thermal density fluctuations $\delta n_T(\boldsymbol{r})=\delta n(\boldsymbol{r})-\delta n_c(\boldsymbol{r})$ by inserting Eqs. (22) and (11) into Eq. (13), and using Eqs. (11) and (14):

$$\delta n_T(\boldsymbol{r},\omega)=2\frac{g}{\hbar}\int d^3\boldsymbol{r}_1\,\tilde{\chi}^0(\boldsymbol{r},\boldsymbol{r}_1,\omega)\,\delta n(\boldsymbol{r}_1,\omega). \tag{23}$$

Another way to derive this result is to consider the possible diagrams in the linear response function χ_T for the thermal density where χ_T is defined by

$$\delta n_T(\boldsymbol{r})=\int d^3\boldsymbol{r}'\,\chi_T(\boldsymbol{r},\boldsymbol{r}',\omega)\,\delta V(\boldsymbol{r}'), \tag{24}$$

and δV is an additional small perturbation coupling to the density operator.

The only diagrams of our approximation for χ not contributing to χ_T are those which start with the trivial vertex function $\tilde{\Lambda}^0_\alpha=\Phi_0$ on the side coupling to the thermal density fluctuation:

$$\chi_T(\boldsymbol{r},\boldsymbol{r}',\omega)=\int d^3\boldsymbol{r}_1\Big[\tilde{\chi}(\boldsymbol{r},\boldsymbol{r}_1,\omega)-\int d^3\boldsymbol{r}_2\int d^3\boldsymbol{r}_3\times\tilde{\Lambda}^0_\alpha(\boldsymbol{r},\boldsymbol{r}_2,\omega)\tilde{G}_{\alpha,\beta}(\boldsymbol{r}_2,\boldsymbol{r}_3,\omega)\tilde{\Lambda}_\beta(\boldsymbol{r}_3,\boldsymbol{r}_1,\omega)\Big]\times\Big[\delta(\boldsymbol{r}_1-\boldsymbol{r}')+\frac{g}{\hbar}\chi(\boldsymbol{r}_1,\boldsymbol{r}',\omega)\Big], \tag{25}$$

$$=\int d^3\boldsymbol{r}_1\Big[\tilde{\chi}^{(r)}(\boldsymbol{r},\boldsymbol{r}_1,\omega)+\frac{g}{\hbar}\int d^3\boldsymbol{r}_2\tilde{\chi}^0(\boldsymbol{r},\boldsymbol{r}_2,\omega)\tilde{\chi}^{(s)}(\boldsymbol{r}_2,\boldsymbol{r}_1,\omega)\Big]\times\Big[\delta(\boldsymbol{r}_1-\boldsymbol{r}')+\frac{g}{\hbar}\chi(\boldsymbol{r}_1,\boldsymbol{r}',\omega)\Big]. \tag{26}$$

In the previous step we have inserted the expression for $\tilde{\Lambda}^0_\alpha$ given by Eq. (21) into Eq. (25). If we use $\delta V=\int\chi^{-1}\delta n$, we obtain

$$\delta n_T(\boldsymbol{r})=\int d^3\boldsymbol{r}_1\int d^3\boldsymbol{r}'\,\chi_T(\boldsymbol{r},\boldsymbol{r}_1,\omega)\chi^{-1}(\boldsymbol{r}_1,\boldsymbol{r}',\omega)\,\delta n(\boldsymbol{r}')$$
$$=\int d^3\boldsymbol{r}_1\int d^3\boldsymbol{r}_2\int d^3\boldsymbol{r}'\Big[\tilde{\chi}^{(r)}(\boldsymbol{r},\boldsymbol{r}_1,\omega)+\frac{g}{\hbar}\tilde{\chi}^0(\boldsymbol{r},\boldsymbol{r}_2,\omega)\tilde{\chi}^{(s)}(\boldsymbol{r}_2,\boldsymbol{r}_1,\omega)\Big]\times\Big[\chi^{-1}(\boldsymbol{r}_1,\boldsymbol{r}',\omega)+\frac{g}{\hbar}\delta(\boldsymbol{r}_1-\boldsymbol{r}')\Big]\delta n(\boldsymbol{r}'), \tag{27}$$

which reduces in the case of resonance ($\int\chi^{-1}\delta n=0$) to the relation

$$\delta n_T(\boldsymbol{r})=\int d^3\boldsymbol{r}_1\int d^3\boldsymbol{r}'\Big[\tilde{\chi}^{(r)}(\boldsymbol{r},\boldsymbol{r}_1,\omega)+\frac{g}{\hbar}\tilde{\chi}^0(\boldsymbol{r},\boldsymbol{r}',\omega)\tilde{\chi}^{(s)}(\boldsymbol{r},\boldsymbol{r}',\omega)\Big]\frac{g}{\hbar}\delta n(\boldsymbol{r}'). \tag{28}$$

Using $\delta n=\delta n_c+\delta n_T$, the equation for δn_c has the form

$$\delta n_c(\boldsymbol{r})=\int d^3\boldsymbol{r}_1\int d^3\boldsymbol{r}'\Big(\delta(\boldsymbol{r}-\boldsymbol{r}_1)-\frac{g}{\hbar}\tilde{\chi}^0(\boldsymbol{r},\boldsymbol{r}_1,\omega)\Big)\times\tilde{\chi}^{(s)}(\boldsymbol{r}_1,\boldsymbol{r}',\omega)\frac{g}{\hbar}\delta n(\boldsymbol{r}'). \tag{29}$$

From Eq. (28) with Eqs. (20) and (9), it is straightforward to derive the final result $\delta n_T=2(g/\hbar)\int\tilde{\chi}^0\delta n$.

For the purpose of calculating δn_c we need to make additional approximations for the proper self-energies $\tilde{\Sigma}_{\alpha,\beta}$. We restrict ourselves to the proper and irreducible diagrams which (a) are only zero- and one-loop diagrams, (b) are connected with Landau damping (since we neglect the Beliaev damping) and (c) do not contain anomalous Green's functions (Popov approximation).

First we introduce those self-energies $\tilde{\Sigma}^0_{\alpha,\beta}$ appearing in the Gross-Pitaevskii-equation for the condensate,

$$\tilde{H}_0\Phi_0(\boldsymbol{r})=0, \tag{30}$$

where $\tilde{H}_0$ is given by

$$\tilde{H}_0=-\frac{\hbar^2}{2m}\Delta+U(\boldsymbol{r})-\mu+g|\Phi_0(\boldsymbol{r})|^2+2gn_T(\boldsymbol{r}), \tag{31}$$

$$\tilde{\Sigma}^0_{\alpha,\beta}(\boldsymbol{r},\boldsymbol{r}',\omega)=[g|\Phi_0(\boldsymbol{r})|^2+2gn_T(\boldsymbol{r}_1)]\begin{pmatrix}1&0\\0&1\end{pmatrix}. \tag{32}$$

They contain the zero-loop diagram $g|\Phi_0(\boldsymbol{r})|^2$ together with the contributions from the stationary density of the noncondensed atoms:

$$n_T(\boldsymbol{r})=\langle\hat{\Phi}^\dagger(\boldsymbol{r})\hat{\Phi}(\boldsymbol{r})\rangle. \tag{33}$$

This density can be calculated in two different ways: either in the Popov approximation as in Ref. [25], which is a self-

consistent, gapless approximation, but does not satisfy the Ward identities in the homogeneous case; or by using the Hartree-Fock approximation, which neglects the quasiparticle aspects of the thermal excitations but has the great virtue of satisfying the Ward identities in the spatially homogeneous case [26] and consequently in the local-density approximation to be used later on. Therefore, we choose this second method in the following. However, it is remarkable that the final results for the shifts and widths we obtain are very similar for both methods of calculating n_T. Due to conditions (a)–(c) we are left with only four additional self-energy contributions which, using the same T-matrix approximation as before, can be written as

$$\tilde{\Sigma}^{(1)}_{\alpha,\beta}(\boldsymbol{r},\boldsymbol{r}',\omega)=\hbar\,\sigma(\boldsymbol{r},\boldsymbol{r}',\omega)\begin{pmatrix}1 & 1\\ 1 & 1\end{pmatrix}, \tag{34}$$

with

$$\sigma(\boldsymbol{r},\boldsymbol{r}',\omega)=\frac{g^2}{\hbar^2}\Phi_0(\boldsymbol{r})\tilde{\chi}^{(r)}(\boldsymbol{r},\boldsymbol{r}',\omega)\Phi_0(\boldsymbol{r}')\ . \tag{35}$$

The corresponding Green's functions

$$\tilde{G}^0_{1,2}=\tilde{G}^0_{2,1}=0, \tag{36}$$

$$\tilde{G}^0_{1,1}(\boldsymbol{r},\boldsymbol{r}',\omega)=\tilde{G}^0_{2,2}(\boldsymbol{r}',\boldsymbol{r},-\omega) \tag{37}$$

satisfy

$$(\hbar\omega-\tilde{H}_0)\tilde{G}^0_{1,1}(\boldsymbol{r},\boldsymbol{r}',\omega)=\hbar\,\delta(\boldsymbol{r}-\boldsymbol{r}'), \tag{38}$$

and $\Sigma_{\alpha\beta}\tilde{G}_{\alpha\beta}(\boldsymbol{r},\boldsymbol{r}',\omega)$ is determined by

$$\sum_{\alpha\beta}\tilde{G}_{\alpha\beta}(\boldsymbol{r},\boldsymbol{r}',\omega)=\int d^3\boldsymbol{r}_1\int d^3\boldsymbol{r}_2\sum_{\kappa\lambda}\tilde{G}^0_{\kappa\lambda}(\boldsymbol{r},\boldsymbol{r}_1,\omega)\times\Big(\delta(\boldsymbol{r}_1-\boldsymbol{r}_2)\,\delta(\boldsymbol{r}_2-\boldsymbol{r}')+\sigma(\boldsymbol{r}_1,\boldsymbol{r}_2,\omega)\times\sum_{\alpha\beta}\tilde{G}_{\alpha\beta}(\boldsymbol{r}_2,\boldsymbol{r}',\omega)\Big). \tag{39}$$

Inserting $\tilde{\chi}^{(s)}=\Sigma_{\alpha\beta}\tilde{\Lambda}_\alpha\tilde{G}_{\alpha\beta}\tilde{\Lambda}_\beta$ in Eq. (29) we obtain for $\delta n_c(\boldsymbol{r})$,

$$\delta n_c(\boldsymbol{r})=\int d^3\boldsymbol{r}_1\int d^3\boldsymbol{r}_2\int d^3\boldsymbol{r}_3\frac{g}{\hbar}\tilde{\Lambda}^0_\kappa(\boldsymbol{r})\tilde{G}^0_{\kappa\lambda}(\boldsymbol{r},\boldsymbol{r}_1,\omega)\times\Big[\tilde{\Lambda}_\lambda(\boldsymbol{r}_1,\boldsymbol{r}_2,\omega)\,\delta n(\boldsymbol{r}_2)+\frac{g}{\hbar}\tilde{\Lambda}^0_\lambda(\boldsymbol{r}_1,\boldsymbol{r}_3,\omega)\times\tilde{\chi}^{(r)}(\boldsymbol{r}_3,\boldsymbol{r}_2,\omega)\,\delta n_c(\boldsymbol{r}_2)\Big], \tag{40}$$

which may be rewritten as

$$\delta n_c(\boldsymbol{r})=\int d^3\boldsymbol{r}_1\int d^3\boldsymbol{r}_2\frac{g}{\hbar}\Phi_0(\boldsymbol{r})\sum_{\alpha\beta}\tilde{G}^0_{\alpha\beta}(\boldsymbol{r},\boldsymbol{r}_1,\omega)\Phi_0(\boldsymbol{r}_1)\times\Big[\delta(\boldsymbol{r}_1-\boldsymbol{r}_2)\,\delta n(\boldsymbol{r}_2)+\frac{g}{\hbar}\tilde{\chi}^{(r)}(\boldsymbol{r}_1,\boldsymbol{r}_2,\omega)\times[\delta n(\boldsymbol{r}_2)+\delta n_c(\boldsymbol{r}_2)]\Big]. \tag{41}$$

To solve Eq. (41) is still very difficult. Instead, we follow the procedure applied in Ref. [13], where the term $(g/\hbar)\tilde{\chi}^{(r)}$ was treated as a small perturbation and the excitation frequencies were determined using first-order perturbation theory. In the perturbation term $(g/\hbar)\tilde{\chi}^{(r)}$ we may replace $\tilde{\chi}^{(r)}$ by $\tilde{\chi}^0$ and δn_c by δn to first order. We then use Eq. (23) to obtain

$$\delta n_c(\boldsymbol{r})=\int d^3\boldsymbol{r}_1\frac{g}{\hbar}\Phi_0(\boldsymbol{r})\sum_{\alpha\beta}\tilde{G}^0_{\alpha\beta}(\boldsymbol{r},\boldsymbol{r}_1,\omega)\Phi_0(\boldsymbol{r}_1)\times[\delta n_c(\boldsymbol{r}_1)+2\,\delta n_T(\boldsymbol{r}_1)]\ . \tag{42}$$

In the next step we show that the unperturbed problem

$$\delta n^0_c(\boldsymbol{r})=\frac{g}{\hbar}\int d^3\boldsymbol{r}_1\Phi_0(\boldsymbol{r})\sum_{\alpha\beta}\tilde{G}^0_{\alpha\beta}(\boldsymbol{r},\boldsymbol{r}_1,\omega)\Phi_0(\boldsymbol{r}_1)\,\delta n^0_c(\boldsymbol{r}_1) \tag{43}$$

is equivalent to the Hartree-Fock-Bogoliubov-Popov calculation of δn^0_c. By dividing Eq. (42) on both sides with the condensate function $\Phi_0(\boldsymbol{r})$, and afterwards muliplying both sides from the left with $(\hbar\omega-\tilde{H}_0)(-\hbar\omega-\tilde{H}_0)$ we derive an equation of the form of the diagonalized HFBP equations:

$$[\tilde{H}^2_0(\boldsymbol{r})-\hbar^2\omega^2]\frac{\delta n_c(\boldsymbol{r})}{\Phi_0(\boldsymbol{r})}=-2g\tilde{H}_0(\boldsymbol{r})n_c(\boldsymbol{r})\times\Big(\frac{\delta n_c(\boldsymbol{r})}{\Phi_0(\boldsymbol{r})}+2\frac{\delta n_T(\boldsymbol{r})}{\Phi_0(\boldsymbol{r})}\Big). \tag{44}$$

This equivalence can be shown by performing the sum and the difference of the Hartree-Fock-Bogoliubov equations:

$$\begin{pmatrix}\tilde{H}^0(\boldsymbol{r})+gn_c(\boldsymbol{r}) & gn_c(\boldsymbol{r})\\ gn_c(\boldsymbol{r}) & \tilde{H}^0(\boldsymbol{r})+gn_c(\boldsymbol{r})\end{pmatrix}\begin{pmatrix}\varphi^{(j)}_1(\boldsymbol{r})\\ \varphi^{(j)}_2(\boldsymbol{r})\end{pmatrix}=\hbar\,\omega^{(j)}_0\begin{pmatrix}\varphi^{(j)}_1(\boldsymbol{r})\\ -\varphi^{(j)}_2(\boldsymbol{r})\end{pmatrix}. \tag{45}$$

We obtain the following diagonalized equations for $\varphi^{(j)}_1\pm\varphi^{(j)}_2$:

$$\hbar^2\omega^{(j)}_0[\varphi^{(j)}_1(\boldsymbol{r})+\varphi^{(j)}_2(\boldsymbol{r})]=[\tilde{H}^2_0(\boldsymbol{r})+2g\tilde{H}_0(\boldsymbol{r})n_c(\boldsymbol{r})]\times[\varphi^{(j)}_1(\boldsymbol{r})+\varphi^{(j)}_2(\boldsymbol{r})] \tag{46}$$

$$\hbar^2\omega_0^{(j)}[\varphi_1^{(j)}(\boldsymbol{r})-\varphi_2^{(j)}(\boldsymbol{r})]=[\tilde{H}_0^2(\boldsymbol{r})+2gn_c(\boldsymbol{r})\tilde{H}_0(\boldsymbol{r})]\times[\varphi_1^{(j)}(\boldsymbol{r})-\varphi_2^{(j)}(\boldsymbol{r})]. \quad (47)$$

If we set $\delta n_T=0$ (unperturbed case) in Eq. (44), we recover the HFBP equation where ω_0 corresponds to the eigenvalues $\omega_0=\omega_0^{(j)}$ and δn_c^0 to the corresponding eigenfunctions $\delta n_c^0=\xi_0^{(j)}=\Phi_0(\varphi_1^{(j)}+\varphi_2^{(j)})$.

The first-order correction due to the dynamics of the thermal density δn_T (or, in other words, due to the existence of $\tilde{\chi}^0$) can be calculated by expanding

$$\delta n_c=\delta n_c^0+\delta n_c^1+\cdots, \quad (48)$$

$$\omega=\omega_0+\omega_1+\cdots, \quad (49)$$

where δn_c^1 and ω_1 are the first order corrections. Inserting this perturbation ansatz into Eq. (44), the first-order contributions must satisfy the equation

$$[\tilde{H}_0^2(\boldsymbol{r})+2g\tilde{H}_0(\boldsymbol{r})n_c(\boldsymbol{r})-\hbar^2\omega_0^2]\frac{\delta n_c^1(\boldsymbol{r})}{\Phi_0(\boldsymbol{r})}=2\hbar^2\omega_1\omega_0\frac{\delta n_c^0(\boldsymbol{r})}{\Phi_0(\boldsymbol{r})}-4g\tilde{H}_0(\boldsymbol{r})n_c(\boldsymbol{r})\frac{\delta n_T(\boldsymbol{r})}{\Phi_0(\boldsymbol{r})}. \quad (50)$$

Multiplying this equation from the left with $[\varphi_1(\boldsymbol{r})-\varphi_2(\boldsymbol{r})]$ and integrating over space, the left side of the equation vanishes. Due to the normalization condition $\int d^3\boldsymbol{r}[\varphi_1(\boldsymbol{r})-\varphi_2(\boldsymbol{r})][\varphi_1(\boldsymbol{r})+\varphi_2(\boldsymbol{r})]=1$ and the relation $\tilde{H}_0(\varphi_1-\varphi_2)=\hbar\omega_0(\varphi_1+\varphi_2)$, we obtain the following result for ω_1:

$$\hbar\omega_1=2g\int d^3r\ \delta n_c^*(\boldsymbol{r})\delta n_T(\boldsymbol{r}) \quad (51)$$

$$=\frac{4g^2}{\hbar}\int d^3r\int d^3r'\ \delta n_c^*(\boldsymbol{r})\tilde{\chi}^0(\boldsymbol{r},\boldsymbol{r}',\omega_0)\delta n_c(\boldsymbol{r}'). \quad (52)$$

This is one of the basic results used in the following for the calculation of shifts and widths of collective excitations. The consistency condition for the applicability of perturbation theory is that $\omega_0\gg|\omega_1|$ must hold, which we shall check below.

Next, let us concentrate on the quantity $\tilde{\chi}^0(\boldsymbol{r},\boldsymbol{r}',\omega_0)$. If one expresses $G_{1,1}^{HF}(\boldsymbol{r},\boldsymbol{r}',i\omega_n)$ in terms of the eigenvalues and eigenvectors of the Hartree-Fock operator H^{HF} ($H^{HF}\varphi_i^{HF}=\varepsilon_i^{HF}\varphi_i^{HF}$),

$$G_{1,1}^{HF}(\boldsymbol{r},\boldsymbol{r}',i\omega_n)=\sum_i\frac{\varphi_i^{HF}(\boldsymbol{r})\varphi_i^{HF*}(\boldsymbol{r}')}{i\omega_n-\varepsilon_i^{HF}/\hbar}, \quad (53)$$

then the standard Matsubara sum in Eq. (15) can be easily performed:

$$\tilde{\chi}^0(\boldsymbol{r},\boldsymbol{r}',i\omega_n)=\sum_{i,j}[n(\varepsilon_j^{HF})-n(\varepsilon_i^{HF})]\times\frac{\varphi_i^{HF}(\boldsymbol{r})\varphi_i^{HF*}(\boldsymbol{r}')\varphi_j^{HF}(\boldsymbol{r}')\varphi_j^{HF*}(\boldsymbol{r})}{i\omega_n-(\varepsilon_i^{HF}-\varepsilon_j^{HF})/\hbar}, \quad (54)$$

where $n(\varepsilon_i^{HF})$ is the Bose factor. From the form of the denominator it is clear that we treat processes leading to Landau damping, but not to Beliaev damping. In calculating the retarded function $\tilde{\chi}^0$ via the analytic continuation $i\omega_n\rightarrow\omega_0+i\eta$ its imaginary part contains a series of Dirac δ peaks due to the discrete spectrum of H^{HF}. In order to obtain finite damping [i.e., the finite imaginary part of ω_1 in Eq. (52)], which was measured in experiments, one needs some smoothing over the Dirac δ peaks. In principle, for the shift there is no need for smoothing, but one must use the same procedure both for the real and imaginary part of $\tilde{\chi}^0$, otherwise they do not fulfill the Kramers-Kronig relations. The smoothing is done by using the semiclassical or local density approximation. First, we calculate the semiclassical Green's function. To do this, let us consider the representation of the Green's function in the center-of-mass, $\boldsymbol{k}$ representation, defined as

$$G_{1,1}^{HF}(\boldsymbol{r},\boldsymbol{r}',\omega)=\int\frac{d^3k}{(2\pi)^3}e^{i\boldsymbol{k}(\boldsymbol{r}-\boldsymbol{r}')}G_{1,1}^{HF}((\boldsymbol{r}+\boldsymbol{r}')/2,\boldsymbol{k},\omega). \quad (55)$$

For this representation the semiclassical Green's function is simply

$$G_{1,1}^{HF(sc)}(\boldsymbol{R},\boldsymbol{k},i\omega_n)=\frac{\hbar}{i\hbar\omega_n-[\epsilon_{\boldsymbol{k}}-\mu(\boldsymbol{R})]}, \quad (56)$$

where

$$\epsilon_{\boldsymbol{k}}=\frac{\hbar^2k^2}{2m},\quad \mu(\boldsymbol{R})=\mu-U(\boldsymbol{R})-2gn_c(\boldsymbol{R})-2gn_T(\boldsymbol{R}). \quad (57)$$

It is easy to show that if one uses the mixed representation for $\tilde{\chi}^0$, similarly defined as in Eq. (55),

$$\tilde{\chi}^0(\boldsymbol{r},\boldsymbol{r}',\omega)=\int\frac{d^3k}{(2\pi)^3}e^{i\boldsymbol{k}(\boldsymbol{r}-\boldsymbol{r}')}\tilde{\chi}^0((\boldsymbol{r}+\boldsymbol{r}')/2,\boldsymbol{k},\omega) \quad (58)$$

then in the new representation Eq. (15) takes the form

$$\tilde{\chi}^0(\boldsymbol{R},\boldsymbol{k},i\omega_n)=-\frac{1}{\beta\hbar}\sum_p\int\frac{d^3k'}{(2\pi)^3}\times G_{1,1}^{HF}(\boldsymbol{R},\boldsymbol{k}+\boldsymbol{k}',i\omega_p)G_{1,1}^{HF}(\boldsymbol{R},\boldsymbol{k}',i\omega_p-i\omega_n). \quad (59)$$

Performing the Matsubara sum, but now with the semiclassical Green's function (56), after the analytic continuation we arrive at

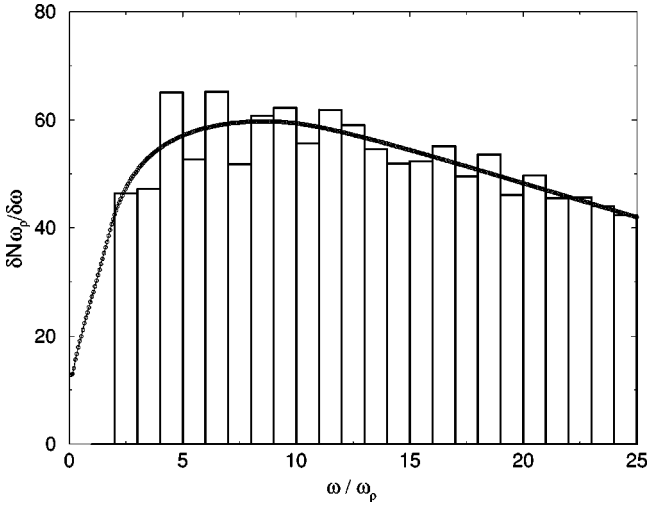

FIG. 1. Spectral contributions to the thermally excited atoms $(dN/d\omega)(\omega)$ as a function of the frequency ω. We compare the result of the local density approximation (open circles) with the histograms from the direct diagonalization for $T=95$ nK and $N_c=7500$.

$$\tilde{\chi}^0(\boldsymbol{R},\boldsymbol{k},\omega)=\int \frac{d^3k'}{(2\pi)^3}\frac{n_{\boldsymbol{k}'}-n_{\boldsymbol{k}+\boldsymbol{k}'}}{\omega-(\epsilon_{\boldsymbol{k}+\boldsymbol{k}'}-\epsilon_{\boldsymbol{k}'})/\hbar+i\eta}, \quad (60)$$

where $n_{\boldsymbol{k}}$ is the Bose factor appearing in the semiclassical (or local-density) approximation:

$$n_{\boldsymbol{k}}=\frac{1}{\exp\left[\beta\left(\frac{\hbar^2k^2}{2m}-\mu(\boldsymbol{R})\right)\right]^{1/2}-1}. \quad (61)$$

In the region where the condensate density vanishes, the condition $\mu(\boldsymbol{R})\approx 0$ holds. As a result, in our semiclassical approximation we would there obtain a logarithmic singularity of $\tilde{\chi}^0(\boldsymbol{R},\boldsymbol{k},w)$ at $k=|\boldsymbol{k}|=\sqrt{2m\hbar\omega}$ leading to large contributions from frequencies around zero, which are completely artificial, since the trapped system has no levels below a certain lowest-lying level. We therefore suppress these unphysical logarithmically singular contributions by choosing the lowest-lying energy level $\omega_{min}=2.12\omega_\rho$ of the Hartree-Fock operator as a natural lower-energy cutoff in our application of the Hartree-Fock and local density approximation. Here ω_ρ is the smallest trap frequency. We thus ensure that all the contributions to frequency shifts and damping rates come only from interactions with modes in the physical energy region above this lowest Hartree-Fock energy level. In Fig. 1 we plot the spectral contributions to the thermally excited atoms as a function of the frequency for both the local-density approximation and the histogram of energy levels obtained by the direct diagonalization of the Hartree-Fock Hamiltonian. The agreement above our cutoff proves to be rather good so that we can expect to obtain reliable results in the local density approximation. With this cutoff the imaginary part of $\tilde{\chi}^0$ becomes

$$\mathrm{Im}\,\tilde{\chi}^{(r)}(\boldsymbol{R},\boldsymbol{k},\omega)=\frac{m^2}{\pi\hbar^3k\beta}\times\ln\left[\frac{1-\exp\left[-\beta\left(\frac{(\hbar\omega-\epsilon_{\boldsymbol{k}})^2}{4\epsilon_{\boldsymbol{k}}}-\mu(\boldsymbol{R})\right)\right]}{1-\exp\left[-\beta\left(\frac{(\hbar\omega+\epsilon_{\boldsymbol{k}})^2}{4\epsilon_{\boldsymbol{k}}}-\mu(\boldsymbol{R})\right)\right]}\right] \quad (62)$$

for $[(\omega m/\hbar k)-(k/2)]^2\geqslant\max(2m\hbar^{-2}[\mu(\boldsymbol{R})+\hbar\omega_{min}],0)$. In the opposite case, due to the cutoff, we have the expression

$$\mathrm{Im}\,\tilde{\chi}^{(r)}(\boldsymbol{R},\boldsymbol{k},\omega)=\frac{m^2}{\pi\hbar^3k\beta}\ln\left[\frac{1-\exp(-\beta\hbar\omega_{min})}{1-\exp[-\beta\hbar(\omega_{min}+\omega)]}\right] \quad (63)$$

for $[(\omega m/\hbar k)-(k/2)]^2\leqslant\max(2m\hbar^{-2}[\mu(\boldsymbol{R})+\hbar\omega_{min}],0)$. After performing the principal value integral, the real part can be written as

$$\mathrm{Re}\,\tilde{\chi}^{(r)}(\boldsymbol{R},\boldsymbol{k},\omega)=\frac{m}{\pi^2\hbar k}\int_{\hbar\sqrt{2m\epsilon(\boldsymbol{R})}}k'\,dk'\,n_{\boldsymbol{k}}\times\ln\left[\frac{a(k,k',\omega,\boldsymbol{R})b(k,k',\omega,\boldsymbol{R})}{c(k,k',\omega)d(k,k',\omega)}\right], \quad (64)$$

with

$$a(k,k',\omega,\boldsymbol{R})=\max\left[\frac{k^2}{2m}-\frac{kk'}{m},\frac{\epsilon(\boldsymbol{R})}{\hbar^2}-\frac{k'^2}{2m}\right]-\hbar^{-1}\omega,$$

$$b(k,k',\omega,\boldsymbol{R})=\min\left[\frac{kk'}{m}-\frac{k^2}{2m},\frac{k'^2}{2m}-\frac{\epsilon(\boldsymbol{R})}{\hbar^2}\right]-\hbar^{-1}\omega,$$

$$c(k,k',\omega)=\frac{k^2}{2m}+\frac{kk'}{m}-\hbar^{-1}\omega,$$

$$d(k,k',\omega)=-\frac{k^2}{2m}-\frac{kk'}{m}-\hbar^{-1}\omega.$$

$\epsilon(\boldsymbol{R})$ is an abbreviation for $\epsilon(\boldsymbol{R})=\max[\mu(\boldsymbol{R})+\hbar\omega_{min},0]$.

III. NUMERICAL METHODS

In our perturbative calculation of ω_1 we should solve first the unperturbed problem for ω_0 and $\delta n_c(\boldsymbol{r})$. This step requires solving the Gross-Pitaevskii (GP) and the HFBP equations. We already have reported on our self-consistent algorithm in Ref. [25] for this problem, which solves the GPE for $\Phi_0(\boldsymbol{r})$ and for the chemical potential using multigrid methods, while the HFBP equations are solved in a large truncated basis. As a result, we have all the necessary inputs, namely, $\Phi_0(\boldsymbol{r})$, $\varphi_1(\boldsymbol{r})+\varphi_2(\boldsymbol{r})$, ω_0, and $n_T(\boldsymbol{r})$ for performing the second step: the use of Eq. (52) in connection with the

retarded density autocorrelation functions [Eqs. (58) and (60)].

This step is straightforward, but from a numerical point of view it requires coping with six-dimensional space integrals and three-dimensional momentum integrals. To reduce the number of numerical integrations we proceed as follows. If we introduce C as an intermediate quantity for

$$C(\boldsymbol{R},\boldsymbol{k})=\int d^3r\, e^{-i\boldsymbol{k}\boldsymbol{r}}\delta n_c^*\left(\boldsymbol{R}-\frac{\boldsymbol{r}}{2}\right)\delta n_c\left(\boldsymbol{R}+\frac{\boldsymbol{r}}{2}\right), \quad (65)$$

then Eq. (52) can be written as

$$\hbar\omega_1=4\frac{g^2}{\hbar}\int d^3R\int\frac{d^3k}{(2\pi)^3}\tilde{\chi}^0(\boldsymbol{R},-\boldsymbol{k},\omega_0)C(\boldsymbol{R},\boldsymbol{k}). \quad (66)$$

Next, let us expand $\delta n_c(\boldsymbol{r})=\Phi_0(\boldsymbol{r})[\varphi_1(\boldsymbol{r})+\varphi_2(\boldsymbol{r})]$ in some *isotropic* harmonic-oscillator basis as

$$\delta n_c(\boldsymbol{r})=\Phi_0(\boldsymbol{r})[\varphi_1(\boldsymbol{r})+\varphi_2(\boldsymbol{r})]=\sum A_i f_i(\boldsymbol{r}), \quad (67)$$

where the set of basis functions $f_i(\boldsymbol{r})$ have the same angular momentum quantum number and parity with respect to reflection on the x-y plane as the unperturbed elementary excitation in question. The next task is to find a connection formula, which transforms any product $f_i^*(\boldsymbol{r})f_j(\boldsymbol{r}')$ to a mixed $(\boldsymbol{R},\boldsymbol{k})$ representation. This step requires some straightforward but rather lengthy calculation, but the advantage we gain is that, due to the facts that $\tilde{\chi}^{(r)}(\boldsymbol{R},\boldsymbol{k},\omega_0)$ is axially symmetric in $\boldsymbol{R}$ for an axially symmetric harmonic-oscillator trap potential and isotropic in $\boldsymbol{k}$ we can perform the integrations over the azimuthal angle of $\boldsymbol{R}$ and over the angles of $\boldsymbol{k}$ in Eq. (66). At the end, apart from discrete sums, we have two spatial integrals in the radial and in the z directions of $\boldsymbol{R}$ and one momentum integral for the imaginary part and two subsequent momentum integrals for the real part of ω_1. Of course, the remaining integrals must be performed numerically.

The form of the above mentioned connection formula which we actually used is based on the following facts: First, the product $f_i^*(\boldsymbol{r})f_j(\boldsymbol{r}')$ is a solution of the two-body, noninteracting harmonic-oscillator problem, which is also separable in center-of-mass and relative coordinates. Thus, expanding it in the other basis containing products of harmonic oscillator wave-functions depending on $\boldsymbol{R}=(\boldsymbol{r}+\boldsymbol{r}')/2$ and $\boldsymbol{r}-\boldsymbol{r}'$, the expansion will contain only a finite number of new basis functions from the energy shell $\varepsilon_i+\varepsilon_j$. Second, the Fourier transform of the harmonic-oscillator wave functions (which we must perform with respect to the relative coordinates) are basically the same as in real space.

IV. RESULTS

We present our numerical results in a way which is directly comparable with the measurement [4]. In Figs. 2 and 3 we put on the horizontal axes $T'=T/T_c$ where T_c is the Bose-Einstein condensate transition temperature for the harmonically trapped ideal gas, and is also the same quantity used in Fig. 1 of Ref. [4]. From that figure we take the same $T=T(T')$ and $N_0=N_0(T')$, which were determined experimentally. Also the same anisotropy ω_z/ω_0 as in the experiment was used. We present our results as a function of the experimental T' because different experimental points belong to different physical conditions since neither N nor N_0 could be kept fixed in the experiment.

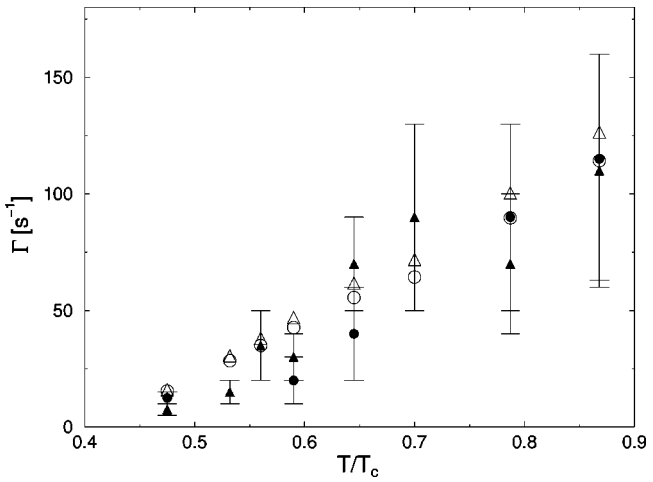

FIG. 2. Damping rates of the $m=0$ (triangles) and $m=2$ (circles) modes as a function of T/T_c. Experimental values (full symbols) with error bars are taken from Fig. 3 of Ref. [4]. Open symbols denote the theoretical predictions Im ω_1 of our model calculation using the dielectric formalism.

In Fig. 2 we plot the imaginary part of ω_1 together with the measured damping rates for the $m=0,2$ modes. For temperatures $T>0.6T_c$, where the Landau damping arising from the bubble graph $\tilde{\chi}^0(\boldsymbol{r},\boldsymbol{r}',\omega)$ is the dominant process, our results are inside the error bars. At lower temperatures the calculated damping rates are slightly above the measured ones. The values for the damping rates due to our model calculation are larger with a factor of $32/9\pi$ compared with

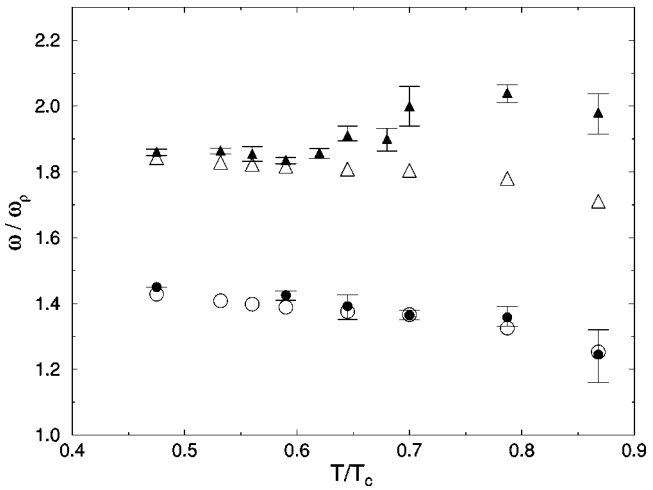

FIG. 3. Excitation frequencies for the $m=0$ and 2 modes as a function of T/T_c. Notations for the experimental values are the same as in Fig. 2. Open symbols denote our theoretical values $\omega_0+\mathrm{Re}\,\omega_1$ in units of the axial trap frequency.

the treatment of all Beliaev graphs to second order [16]. This is not surprising, because the neglection of the Beliaev damping and the use of local-density approximation is only justified for temperatures satisfying the condition $k_B T \gg \mu$, only valid for $T \gg 0.6 T_c$. The same condition is necessary to neglect the quasiparticle character of the additional excited particles contributing to the self-energies via scattering processes. Comparing our results for the damping rates with the values of the unperturbed ω_0 it is manifest that $\mathrm{Im}\,\omega_1 \ll \omega_0$. The real part of ω_1 is also much smaller than ω_0 for all the calculated points. Therefore, the criterium for the applicability of perturbation theory is justified.

In Fig. 3 we plot $\omega_0 + \mathrm{Re}\,\omega_1$ together with the experimentally measured frequencies. For $m=2$ we have good agreement for temperatures above $T \gtrsim 0.6 T_c$, and slightly larger negative shifts compared to the experimental values below $T = 0.6 T_c$. The results for the $m=0$ mode show the same slight difference in the low-temperature region. But approaching higher temperatures the experimental and the numerical results predict a different behavior for the excitation energies. While experimentally they are increasing we found decreasing values in our model calculation. The same qualitative discrepancy was also found by Hutchinson *et al.* in Ref. [22] using a different approach to the problem. They also reported good agreement with the measured frequencies for $m=2$, but disagreement for $m=0$. A possible explanation for the above discrepancies was given by Bijlsma and Stoof in Ref. [23], who used the quantum Boltzmann equation in the collisionless regime and calculated low-lying excitation frequencies using a variational approach for the $m=0$ and 2 modes. They found that there are two nearby $m=0$ modes, one of them describing the in-phase oscillations and the other one the out-of-phase oscillations of the condensate and thermal cloud. They concluded that it might be possible that in the experiment both $m=0$ modes are excited together, and that in Ref. [4] only the upper one or a superposition of both might be plotted. If there are two nearby $m=0$ modes we must explain why in our calculation we have obtained only one of them (and furthermore not the experimentally measured one). It is clear that by our perturbative treatment we fixed ourselves to one of them by calculating the corrections to the Hartree-Fock-Bogoliubov-Popov equations for $\delta n_T \ll \delta n_c$, and we followed it in changing the temperature. Our results correspond to the branch describing the out-of-phase motion calculated in Refs. [23,24]. To see this we recall our formula for the corrections $\omega_1 = 2g \int d^3r\, \delta n_c^*(\boldsymbol{r}) \delta n_T(\boldsymbol{r})$, and the fact that ω_1 is found to be negative in our results. Therefore, the spacial average over the amplitude product of δn_T and δn_c is negative, which means that δn_T and δn_c are out of phase.

The in-phase mode can accordingly be obtained, if, in fact, there is another nearby $m=0$ mode in our model approximation, if we do not use perturbation theory for solving Eq. (44). Instead we should consider the eigenvalues of the bubble graph $\tilde{\chi}^0$ corresponding to the thermal density fluctuation δn_T, and calculate their perturbation due to δn_c. This possibility was supported by an early study of the behavior of the poles of the density-density autocorrelation function in the homogeneous Bose gas [11], where it was shown that there are more, but purely damped, modes. They remain purely overdamped above T_c in accord with a recent experiment [27]. It can be shown that one of the overdamped damped modes corresponds to $\delta n_T \gg \delta n_c$ and that it is a mode where δn_T and δn_c relax out of phase [28]. In addition it is clear that in a harmonic trapping potential these damped modes will acquire a nonzero real part of their oscillation frequency. However, to really demonstrate this for the eigensolutions of the density-density autocorrelation function in the inhomogeneous case, and furthermore to show that in this case the missing mode can be described in this way, requires further analytical and numerical studies.

V. CONCLUSIONS AND FURTHER REMARKS

In this paper we have investigated the predictions of the dielectric formalism applied to the model of a Bose gas obtained by extending simpler models discussed in the literature [7,11,13]. The proper and irreducible building blocks $\tilde{\chi}^{(r)}$ and $\tilde{\Lambda}$ are already the result of summing up higher-order contributions in the form of a ladder approximation that only sums up geometric series of the bubble graph $\tilde{\chi}^0$. From the second-order Beliaev diagrams, for the irreducible self-energies we keep only those which are supposed to give large contributions. Since Landau damping dominates Beliaev damping in the temperature region $T \gtrsim 0.6 T_c$ of the measurement at JILA, we neglect the diagrams connected with Beliaev damping. We reduce the amount of diagrams further to only zero- and one-loop diagrams. In addition, we neglect all the self-energy diagrams containing anomalous Green's functions. To find poles of the density-density correlation function, i.e., collective excitations, we used first-order perturbation theory, where the proper and regular part of the density-density correlation function played the role of the perturbing operator. We showed that the physical content of the unperturbed problem is equivalent to finding elementary excitations in the Hartree-Fock-Bogoliubov-Popov approximation. The fact that all first-order corrections to the Hartree-Fock-Bogoliubov-Popov equations can be described with one bubble graph $\tilde{\chi}^0$ permits us to draw conclusions about the behavior of the quantities δn_c and δn_T from our numerical results. Due to the negative energy shifts obtained in our numerical results, we can identify their motion to be out of phase. Since we establish our model on the basis of a dielectric formalism, we achieve the required correspondence of the spectra of the Green's functions and the density autocorrelation function, ensuring gapless spectra of quasiparticle modes and density modes in the homogeneous limit. The version [Eq. (42)] of our equation (41) agrees with the dynamic Hartree-Fock-Bogoliubov-Popov theory presented by Minguzzi and Tosi [14]. They derived Eq. (42) by linearizing the time-dependent Gross-Pitaevskii equation around its stationary solution $n(\boldsymbol{r},t) = n_c(\boldsymbol{r}) + \delta n_c(\boldsymbol{r},t)$, and Eq. (23) by an equivalent linearization of the Hartree-Fock equation for the noncondensate field operator. The bubble graph $\tilde{\chi}^0$ connected with Eq. (23) is also a product of Green's functions in Hartree-Fock approximation in their theory.

Bijlsma and Stoof [23] also considered Eq. (23), and used the dispersion relation of the Hartree-Fock operator in the local-density approximation for their calculations. In contrast to us, they examined the collisionless Boltzmann equation for the Wigner function, and solved the equations with a variational approach, which cannot describe any damping of the excitations. Whereas the local-density approximation we (and the authors of Ref. [23]) use is better for large condensates, the approach of Fedichev *et al.* [20] is better suited for the opposite case of small condensates due to the assumption of hard chaos, which can only be fulfilled for small condensates. In this approach the diagrams are evaluated by integrating along the classical trajectories.

We have found good agreement both for the shift and the damping with the experiment for $m=2$, and also for the damping rate of the $m=0$ mode, but disagreement similar to that of Ref. [22] in the frequency shift for the $m=0$ mode. We explained this discrepancy with observation by an artifact of our perturbative treatment, and by applying the argument of Refs. [23,24], namely, by supposing another nearby lying $m=0$ mode.

To decide whether a nonperturbative treatment of the problem, still within the framework of our model approximation, can show the existence of the missing $m=0$ mode requires an extended numerical study. Our future plan is to find the poles in a nonperturbative way, and study the decoupling of the single particle and the collective excitations for $T \rightarrow T_c - 0$, along the lines of the calculation for homogeneous system of Ref. [11]. A further natural extension of this work could be to study further and more difficult, but still numerically manageable, model approximations.

ACKNOWLEDGMENTS

We would like to thank Gy. Bene and M. Fliesser for many stimulating discussions. This work was supported by a project of the Hungarian Academy of Sciences and the Deutsche Forschungsgemeinschaft under Grant No. 95. R.G. and J.R. wish to acknowledge support by the Deutsche Forschungsgemeinschaft through the Sonderforschungbereich 237 ''Unordnung and große Fluktuationen.'' Two of us (A.Cs. and P.Sz.) would like to acknowledge support by the Hungarian National Scientific Research Foundation under Grant Nos. OTKA T029552, T025866, and F020094, and by the Ministry of Education of Hungary under Grant No. FKFP1059/1997.

[1] E. A. Cornell, J. R. Ensher, and C. E. Wiemann, preprint, cond-mat/9903109.
[2] W. Ketterle, D. S. Durfee, and D. M. Stamper-Kurn, preprint, cond-mat/9904034.
[3] D. S. Jin, J. R. Ensher, M. R. Matthews, C. E. Wiemann, and E. A. Cornell, Phys. Rev. Lett. **77**, 420 (1996).
[4] D. S. Jin, M. R. Matthews, J. R. Ensher, C. E. Wiemann, and E. A. Cornell, Phys. Rev. Lett. **78**, 764 (1997).
[5] M. O. Mewes, M. R. Andrews, N. J. van Drouten, D. M. Kurn, C. G. Townsend, and W. Ketterle, Phys. Rev. Lett. **77**, 988 (1996).
[6] D. M. Stamper-Kurn, H.-J. Miesner, S. Innouye, M. R. Andrews, and W. Ketterle, Phys. Rev. Lett. **81**, 500 (1998).
[7] A. Griffin, *Excitations in a Bose-Condensed Liquid* (Cambridge University Press, Cambridge, 1993).
[8] Shang-Keng Ma and Chia-Wei Woo, Phys. Rev. **159**, 165 (1967).
[9] I. Kondor and P. Szépfalusy, Acta Phys. Acad. Sci. Hung. **24**, 81 (1968).
[10] V. K. Wong and H. Gould, Ann. Phys. (N.Y.) **83**, 252 (1974).
[11] P. Szépfalusy and I. Kondor, Ann. Phys. (N.Y.) **82**, 1 (1974).
[12] S. H. Payne and A. Griffin, Phys. Rev. B **32**, 7199 (1985).
[13] Gy. Bene and P. Szépfalusy, Phys. Rev. A **58**, R3391 (1998).
[14] A. Minguzzi and M. P. Tosi, J. Phys. Condens. Matter **9**, 10 211 (1997).
[15] F. Dalvovo, S. Giorgini, L. Pitaevskii, and S. Stringari, Rev. Mod. Phys. **71**, 463 (1999).
[16] H. Shi and A. Griffin, Phys. Rep. **304**, 1 (1998).
[17] W. Vincent Liu, Phys. Rev. Lett. **79**, 4056 (1997).
[18] L. P. Pitaevskii and S. Stringari, Phys. Lett. A **235**, 398 (1997).
[19] S. Giorgini, Phys. Rev. A **57**, 2949 (1998).
[20] P. O. Fedichev, G. V. Shlyapnikov, and J. T. M. Walraven, Phys. Rev. Lett. **80**, 2269 (1998).
[21] P. O. Fedichev and G. V. Shlyapnikov, Phys. Rev. A **58**, 3146 (1998).
[22] D. A. W. Hutchinson, R. J. Dodd, and K. Burnett, Phys. Rev. Lett. **81**, 2198 (1998).
[23] M. J. Bijlsma and H. T. C. Stoof, preprint, cond-mat/9902065.
[24] H. T. C. Stoof, preprint, cond-mat/9812424.
[25] J. Reidl, A. Csordás, R. Graham, and P. Szépfalusy, Phys. Rev. A **59**, 3816 (1999).
[26] M. Fliesser, J. Reidl, P. Szépfalusy, and R. Graham (unpublished).
[27] M. R. Andrews, D. M. Kurn, H.-J. Miesner, D. S. Durfee, C. G. Townsend, S. Inouye, and W. Ketterle, Phys. Rev. Lett. **79**, 553 (1997).
[28] M. Fliesser (private communication).